Histochemistry and Cell Biology
https://doi.org/10.1007/s00418-020-01872-y

ORIGINAL PAPER

Melanoma xenotransplant on the chicken chorioallantoic membrane: a complex biological model for the study of cancer cell behaviour

Karolína Strnadová[1,2] · Michal Španko[1,3] · Barbora Dvořánková[1,2] · Lukáš Lacina[1,2,4] · Ondřej Kodet[1,2,4] · Andrej Shbat[1] · Ivo Klepáček[1] · Karel Smetana Jr.[1,2]

Accepted: 10 March 2020

Abstract

The globally increasing incidence of cancer, including melanoma, requires novel therapeutic strategies. Development of successful novel drugs is based on clear identification of the target mechanisms responsible for the disease progression. The specific cancer microenvironment represents a critically important aspect of cancer biology, which cannot be properly studied in simplistic cell culture conditions. Among other traditional options, the study of melanoma cell growth on the chicken chorioallantoic membrane offers several significant advantages. This model offers increased complexity compared to usual in silico culture models and still remains financially affordable. Using this model, we studied the growth of three established human melanoma cell lines: A2058, BLM, G361. The combination of histology, immunohistochemistry with the application of human-specific antibodies, intravascular injection of contrast material such as filtered Indian ink, Mercox solution and phosphotungstic acid, and X-ray micro-CT and live-cell monitoring was employed. Melanoma cells spread well on the chicken chorioallantoic membrane. However, invasion into the stroma of the chorioallantoic membrane and the limb primordium graft was rare. The melanoma cells also significantly influenced the architecture of the blood vessel network, resulting in the orientation of the vessels to the site of the tumour cell inoculation. The system of melanoma cell culture on the chorioallantoic membrane is suitable for the study of melanoma cell growth, particularly of rearrangement of the host vascular pattern after cancer cell implantation. The system also has promising potential for further development.

Keywords Melanoma · Cancer microenvironment · Cancer-associated fibroblasts · Melanoma invasiveness · Embryo · Chorioallantoic membrane

Introduction

The incidence of malignant melanoma is increasing worldwide at a rate faster than that of other malignant diseases. Until now, the melanoma-associated mortality has remained high in advanced stage patients, despite the enormous efforts and several new therapeutic options (Dvořánková et al. 2017). Similarly to other types of tumours, the microenvironment significantly influences the biological properties of melanoma (Lacina et al. 2015; Dvořánková et al. 2017). Some of the novel successful therapeutic strategies, namely immune checkpoint inhibitors, target the immune mechanisms in the tumour microenvironment and elicit immune clearance of the tumour. However, there are multiple other components beyond immune cells present in the tumour stroma. Their therapeutic potential has not yet been fully revealed and is worthy of scientific attention. The cellular component of the tumour microenvironment mainly

Karolína Strnadová and Michal Španko have contributed equally.

✉ Lukáš Lacina
lukas.lacina@lf1.cuni.cz

✉ Karel Smetana Jr.
karel.smetana@lf1.cuni.cz

[1] Institute of Anatomy, First Faculty of Medicine, Charles University, 12800, Prague, Czech Republic

[2] BIOCEV, First Faculty of Medicine, Charles University, 25250 Vestec, Czech Republic

[3] Department of Stomatology, First Faculty of Medicine, Charles University, 12800, Prague, Czech Republic

[4] Department of Dermatovenereology, First Faculty of Medicine, Charles University, 12808 Prague, Czech Republic

Published online: 30 March 2020

includes cancer-associated fibroblasts, as well as pericytes, endothelial cells, adipocytes, and others. Cancer-associated fibroblasts are the most numerous population, and, therefore, have attracted attention of researchers for many years. However, a significant regulatory function can be executed even by some minor population (Dvořánková et al. 2019).

The cancer microenvironment can be studied in vitro at the 2D or 3D level (Kodet et al. 2015; Jobe et al. 2016, 2018) or in vivo. The traditional cell culture methods based on separated cell types lack the complexity of the tissue microenvironment, which is an indispensable factor for cancer progression in the organism. We can enrich the standard culture model based on malignant cell lines by employing one or more stromal populations simultaneously. Their interactions may occur via direct cell-to-cell contacts or indirectly, via soluble biologically active molecules. Moreover, physiochemical features may also play a significant role in tumour biology. Tissue hypoxia is one of the traditionally extensively studied features (Gaustad et al. 2017), which can also be achieved in experimental in vitro models. However, the complexity of tissue, where multiple cell types interact simultaneously, is not reproduced entirely.

The most frequently used animal model for cancer studies is based on various highly inbred mouse strains. Compared to cell line-based research, murine models offer much higher biological complexity. Immunodeficient mouse models are particularly suitable for cancer research. However, as there is an outstanding diversity in immunodeficient mouse models, it is difficult to choose the most appropriate strain for a particular study. The selection of an immunodeficient mouse strain also brings bias to the studied experimental system. Mice are sometimes not completely reliable as models of human disease, including cancer. In addition, the achieved biological complexity is also associated with a significantly higher price (Pérez-Guijarro et al. 2017). Therefore, a simple and affordable biological model is needed for biomedical research.

It was frequently noted earlier that the chorioallantoic membrane (CAM) of the chicken embryo represents a complex structure with precisely described developmental dynamics. CAM represents a biologically relevant substrate with several cellular components, extracellular matrix and fully functional continuous blood flow. It can be used efficiently for in vitro cultures or for in vivo studies. CAM allows frequent or continuous microscopic evaluation. Finally, CAM offers straightforward interpretation by methods of histology or histochemistry. It is also reasonably cheaper than mouse models.

Ribatti (2016) reviewed various applications of CAM as an excellent tool for the study of many biologically as well as medically relevant problems. Beside traditional studies of angiogenesis, CAM was even used as an in vivo model of implantation of cancer cells, including melanoma (Ribatti 2014; Avram et al. 2017) and metastasising (Cimpean et al. 2008; Deryugina and Quigley 2008; Subauste et al. 2009).

Melanomas are tumours originating from melanocytes, the pigment-producing cells of the skin. The function of melanocytes in the skin is tightly regulated by the target tissue microenvironment. Melanocytes migrate from the neural crest to the skin during embryonic development (Shakhova 2014). Experiments in zebrafish showed that transcription factor crestin is typical of neural crest embryonic cells. Of note, crestin is also significantly activated in malignant melanoma (Kaufman et al. 2016).

When injected to the embryo, melanoma cells colonise similar body sites as the neural crest progeny (Lee et al. 2005; Bailey et al. 2012; Bailey and Kulesa 2014). Even in vitro, conditioned medium from embryonic stem cells influences the phenotype and functional properties of melanoma cells (Kodet et al. 2013). The conditioned medium can be easily used as a tissue microenvironment surrogate. These findings indicate an important effect of the embryonic microenvironment on melanoma cell biology. Furthermore, there is evidence of melanoma cell reprogramming by the embryonic microenvironment and loss of their malignant behaviour (Kasemeier-Kulesa et al. 2008; Díez-Torre et al. 2009).

In the presented study, we evaluated the growth of three melanoma cell lines in the CAM model. We mapped the remodelling of immature vessels in CAM after inoculation of melanoma cells. To study the effects of hypoxic conditions, we also grafted an isolated limb bud onto CAM before melanoma cell implantation. The spatial reorganisation of the CAM vascular pattern was visualised by injections of phosphotungstic acid (PTA), Indian ink, or synthetic resin to the CAM vessels. The melanoma cells used in this study were not chemically labelled to prevent the potential effect of chemical label on their viability and biological properties. We distinguished the grafted melanoma cells in the tissues by a species-specific antibody recognising human vimentin (Vim), enzyme expression (galactosidase), and HMB-45 marker of melanocytes.

Materials and methods

Cell culture and conditioned media preparation

Three invasive melanoma cell lines were tested. Cells of the BLM line were obtained from L. van Kempen and H. Van Krieken from the Department of Pathology, Radboud University (Nijmegen, the Netherlands). G361 and A2058 cell lines were purchased from the American Type Culture Collection. The cells were maintained in DMEM with 10% FBS (Sigma Aldrich, Prague, Czech Republic). LacZ melanoma cell lines tagging was performed according to

the manufacturer's protocol (LV-348, AMS Biotechnology (Europe) Ltd, Abingdon, U.K.) with consequent puromycin selection. As control population, normal human highly pigmented melanocytes (HPM) were obtained from J. Vachtenheim (Institute of Medical Chemistry and Laboratory Medicine, 1st Faculty of Medicine, Charles University, Prague, Czech Republic). HPM melanocytes were maintained in M254 culture medium (Thermo Fisher Scientific, Prague, Czech Republic). Human dermal fibroblasts were prepared from the skin samples of healthy donors with the donor's explicit informed consent and approval by the local ethics committee (Dvořánková et al. 2019). The same procedures were also used to prepare the chicken embryonic fibroblasts from CAM and adult chicken dermal fibroblasts (CDF), which were cultured as described earlier (Dvořánková et al. 2019). Preparation of primary cells was approved by the local ethics committees of the First and Third Faculty of Medicine, Charles University in Prague according to the Declaration of Helsinki as described for use of human material. The characterisation of cells and the cultivation procedure were described in detail by Kodet et al. (2015) and Dvořánková et al. (Jobe et al. 2016; Dvořánková et al. 2019). The conditioned media (CM) were collected from the avian fibroblast monolayers (CAM or CDF) cultured in DMEM with 10% FBS. The medium was changed in fibroblast cultures forming subconfluent layers (70%) and harvested after further 48 h of cultivation. It was filtered (0.2 µm), aliquoted, and stored (at − 80 °C) for later experimental use. All cell lines were routinely tested for Mycoplasma sp. contaminations.

Chick embryo preparation

Fertilised eggs of the Ross 308 hybrid of the chick (*Gallus gallus domestica*; Xaverov, Czech Republic) were incubated in a humidified atmosphere in an incubator at 37.5 °C for 4 days in stage 22–24 according to Hamburger and Hamilton (1992). The eggshell was decontaminated by 70% ethanol (Rugh 1948), and a manipulation window was cut to the eggshell.

In a defined cohort of embryos, the early primordium of the upper limb (HH 23–24) was transplanted to the surface of CAM outside the embryo before the application of cancer cells to mimic a hypoxic niche. After grafting, the fenestration of the eggshell was sealed by paraffin and attached sterile glass (Rugh 1948; Klepáček and Jirsa 1994) and maintained in the incubator. After day 2, the cancer cells were implanted onto the CAM surface. The melanoma cells were seeded as a concentrated suspension onto the surface of CAM in a quantity of 10^6 cells in 10 µl of PBS per embryo. Eggs were further incubated for 2–6 consecutive days. The numbers of embryos used for experimental cohorts are presented in Table 1 (total $n = 45$). All manipulations with embryos were performed using stereomicroscope SMZ 18 (Nikon, Vienna, Austria) using sterile instruments. The experimental design of this study, including both in vitro and *in ovo* studies, is summarised in Fig. 1.

Immunofluorescent and immunohistochemical detection of cancer cells in whole-mount specimens

CAM was dissected from the egg after attachment to a paper frame, which offers stabilisation of the specimen and prevents rolling. CAM was gently rinsed in PBS and briefly fixed in 4% paraformaldehyde (in PBS, pH 7.2, 5 min) and repeatedly gently washed with PBS. The specimens for immunocytochemistry were consequently permeabilised by Tween 20 (Sigma-Aldrich, Prague, Czech Republic) at concentration 0.2% in PBS. Vimentin was detected by specific antibody clone V9 (DAKO, Glostrup, Denmark) (Bohn et al. 1992). The species specificity was verified in human and chicken fibroblasts (Fig. 2a, b) with the employment of appropriate negative controls (either omission of the primary antibody or use of a tissue-irrelevant antibody of the same isotype, isotype control, ThermoFisher Scientific, Prague, Czech Republic). The chicken-reactive vimentin for avian fibroblast phenotype confirmation was mouse monoclonal antibody, clone RV202 (Abcam, Cambridge, UK).

TRITC-labelled goat anti-mouse antibody (Sigma-Aldrich, Prague, Czech Republic) was used as the second step antibody to detect vimentin. Both the first and second step antibodies were diluted as recommended by the supplier. Nuclei were counterstained with 4′,6-diamidine-2′-phenylindole dihydrochloride (DAPI) (Sigma-Aldrich, Prague, Czech Republic). Specimens were mounted as whole mounts to Vectashield (Vector Laboratories, Burlingame,

Table 1 Results of melanoma xenotransplantation on the chick embryo CAM

Cell line	No. of embryos/no. of implants	No. of embryos/invasion to CAM	No. of grafted limb buds/migration to the graft site	No. of limb buds/no. of limbs with cancer cells	No. of embryos/metastases (liver, lung, brain)
A2058	15/15	15/1	5/5	5/1	15/0
BLM	15/15	15/0	5/5	5/0	15/0
G361	15/15	15/1	5/5	5/1	15/0

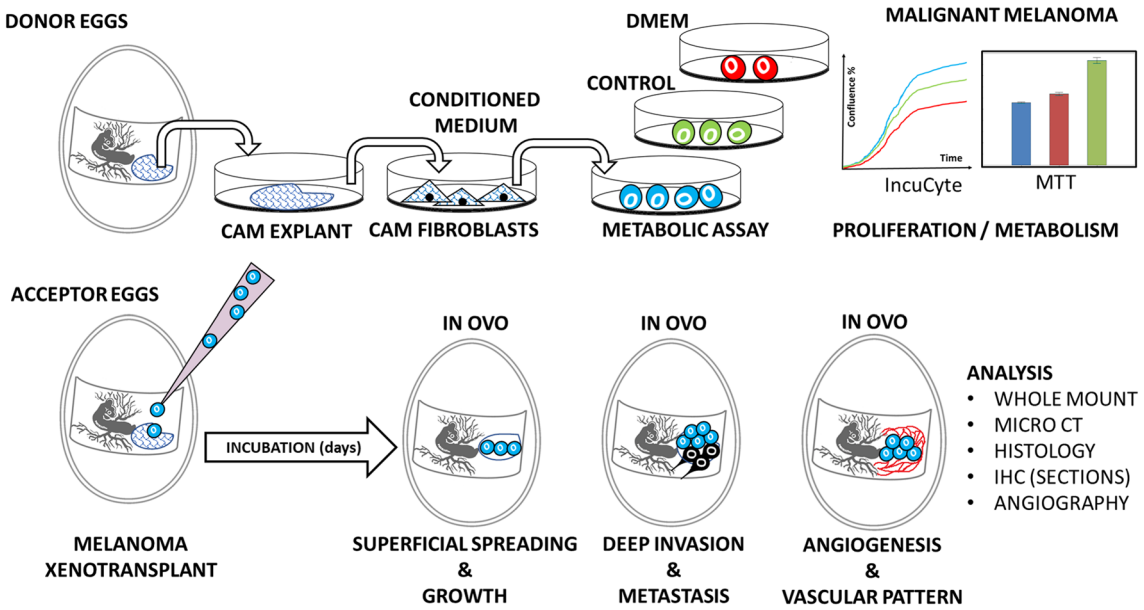

Fig. 1 Experimental workflow. The fibroblasts were isolated from CAM of donor eggs or adult avian skin. The effects of conditioned media on the growth of malignant melanoma cells was tested using the metabolic (MTT) assay and the growth was continuously monitored by microscopy (Incucyte system). Melanoma cells were grafted on the chick chorioallantoic membrane in acceptor eggs. We monitored the melanoma cell spread on the surface or invasion to the chorioallantoic membrane stroma (or into the grafted limb primordia) and changes in the vascular network surrounding the application site

CA, USA) and inspected by an Eclipse 90i microscope (Nikon, Viena, Austria) equipped with NIS-Elements AR.40.00 for data storage and analysis and with a ProgRes MF CCD camera (Jenoptik Optical Systems GmBH, Jena, Germany).

In case of X-Gal reaction for LacZ-tagged melanoma cells, the fixation was shortened to 3 min only. The visualisation was performed using a β-Gal Staining Kit (Invitrogen, Prague, Czech Republic) following the manufacturer's protocol. The documentation in the bright field was performed using a Leica DM 2000 microscope equipped with a digital camera.

Immunohistochemical detection of melanoma cells

Tissue sections (5 µm) were cut from routinely prepared FFPE blocks. Slides were deparaffinised and rehydrated. HBM-45 was selected out of melanoma markers, because this particular antibody does not require any antigen retrieval using heat treatment before staining according to the manufacturer's instructions (MA5-16712, ThermoFisher Scientific, Prague, Czech Republic). Endogenous peroxidase activity was blocked by 1% hydrogen peroxide in PBS (20 min at room temperature), and non-specific interaction of immunoglobulins was blocked by incubation in diluted 10% non-immune goat serum (20 min, room temperature). The incubation with the primary antibody (diluted 1/40 in blocking solution) was performed at 4 °C overnight. The immunohistochemical reaction was visualised using an HRP polymer kit with diaminobenzidine (Histofine Simple Stain MAX PO Multi, Nichirei, Bioscience, Tokyo Japan). The nuclei were counterstained by hematoxylin and specimens were dehydrated, cleared and mounted in synthetic mountant (Jobe et al. 2016). The imaging was performed with a Leica DM 2000 microscope equipped with a digital camera.

Again, the specificity of the reaction was tested by replacement of the specific primary antibodies by a tissue-irrelevant isotype antibody (ThermoFisher Scientific, Prague, Czech Republic).

Detection of vessels by Indian ink, PTA and resin

CAM vessels were injected with filtered Indian ink (Klepáček et al. 1999), PTA (Kokorin and Gudima 1968), or Mercox^{R} II Blue resin (Mercox-Japan Vilene, Tokyo, Japan) and processed as described elsewhere (Navarro et al. 1998; Klepáček et al. 1986). The resin/PTA-injected specimens were inspected and analysed by X-ray micro-CT using a desktop ex vivo device SkyScan1272 with a 16MPx CCD detector (Bruker, Kontich, Belgium). Each specimen was individually placed in a plastic tube with PBS and mounted on a microstage as described. The specimens were scanned in resolution 3280 × 4904 px without employing an X-ray filter. The data were reconstructed using program NRecon and visualised using program CTVox, both obtained from Bruker (Kolesová et al. 2018).

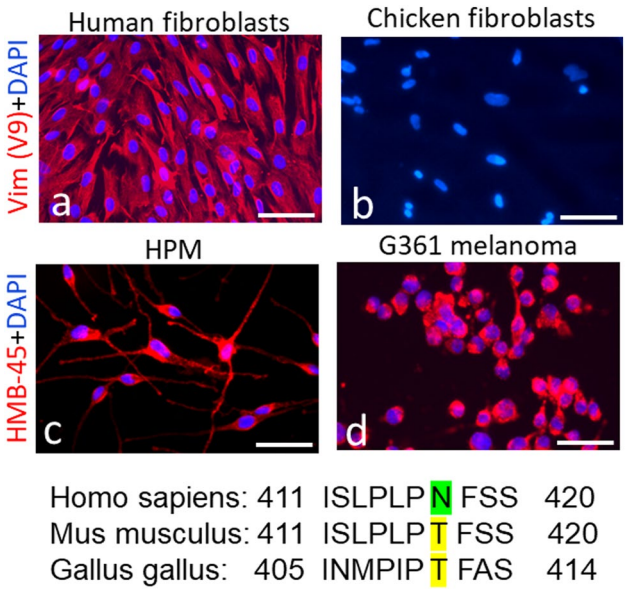

Fig. 2 Detection of human vimentin (V9 clone, red signal) in human dermal fibroblasts (**a**), and absence of V9 staining in chicken embryonic fibroblasts (**b**). Detection of melanocyte marker (HMB-45, red signal) in normal human highly pigmented melanocytes (**c**) and melanoma cells (**d**). Comparison of analogous sequences of human, murine and chicken vimentin (amino acids 411–420 and 405–414, respectively). Asparagine 417 (N) is highlighted in green in the human vimentin (the key structural motif for V9 antibody binding); in contrast, the similarity of murine and chicken vimentin (threonine 417 and 411, respectively) is highlighted in yellow. The human, murine and chicken vimentin sequences were aligned using the https://www.uniprot.org/align/ database tool and according to Kong et al. (2011) and also specifically to Tomiyama et al. (2017) for the purposes of V9 binding motif identification. The bar represents 50 µm

Testing the effect of conditioned media on the growth and metabolic properties of cancer cells

The proliferation kinetics of A2058, BLM and G361 melanoma cells was tested using the IncuCyte ZOOM Kinetic live cell imaging system (Essen BioScience, Ann Arbor, MI, USA) as described earlier (Živicová et al. 2017). The melanoma cells were seeded in low density in 96-well plates. Next day, the standard cultivation medium was replaced by the conditioned medium. The effect of conditioned media prepared from the subconfluent layers of CAM and CDF was measured and expressed as confluence (%). Cultures were screened every 2 h for approximately 9 days. The differences in proliferation were compared at the moment of exponential growth when the first averaged line (representing $n = 12$) met 50% of confluence. The data were analysed using PAST3 software (http://palaeo-electronica.org/2001_1/past/issue1_01.htm); Tukey's Honest Significant Difference test was used to detect statistical significance.

The results were further compared with the evaluation of the metabolic activity of A2058, BLM and G361 melanoma cells under the influence of conditioned media using the MTT test (Stockert et al. 2018) on the 7th day of cultivation, when the growth of the cells was stabilised.

Results

Isolation of chicken dermal and CAM fibroblasts and their effects on melanoma cell line growth

The fibroblasts from the chick chorioallantoic membrane (CAM) were successfully isolated using the explant method following the protocol published earlier by us (Kodet et al. 2013) and phenotype was determined according to our published protocol (Dvořánková et al. 2019). We also isolated chicken dermal fibroblasts (CDF) from avian skin as control cells for this experiment using otherwise identical conditions. The cells were easily expanded in DMEM with 10% FBS for experimental purposes and used before passage No. 5. The immunocytochemical staining with vimentin antibody V9 was negative in all cells of avian origin (Fig. 2). This finding contrasted with the confirmed positive result detected in human cell lines (normal human fibroblasts presented here; the data from melanoma cell lines are not presented). However, vimentin was confirmed in avian fibroblast by staining with alternative mouse monoclonal antibody RV202(data not shown). This contrast also confirms the species specificity of the immunocytochemical reaction of V9 antibody (the negative control is thus not presented here).

The fibroblast-conditioned media (CAF-CM and CDF-CM) significantly increased the proliferation kinetics of all three cancer cell lines when compared to DMEM (p value < 0.008 in all cases). However, a statistically significant difference between CDF-CM and CAM-CM was observed only in the A2058 melanoma cell line (p value 0.002). The trend observed in BLM and G361 melanoma cell line growth was similar, yet not significant (p value 0.24 and 0.15, respectively). We also measured the differences in metabolic activity of melanoma cell lines in different media using the MTT assay. Similarly, A2058 sensibly reflected the difference between CAM-CM vs CDF-CM (p value > 0.001). There was no statistically significant difference between the metabolic rate of BLM and G361 melanoma cell lines in various culture media (Fig. 3).

Observation in ovo

The results of melanoma xenotransplantation are summarised in Table 1. All cell lines used in the experiments formed distinct colonies on the surface of CAM. Colonies

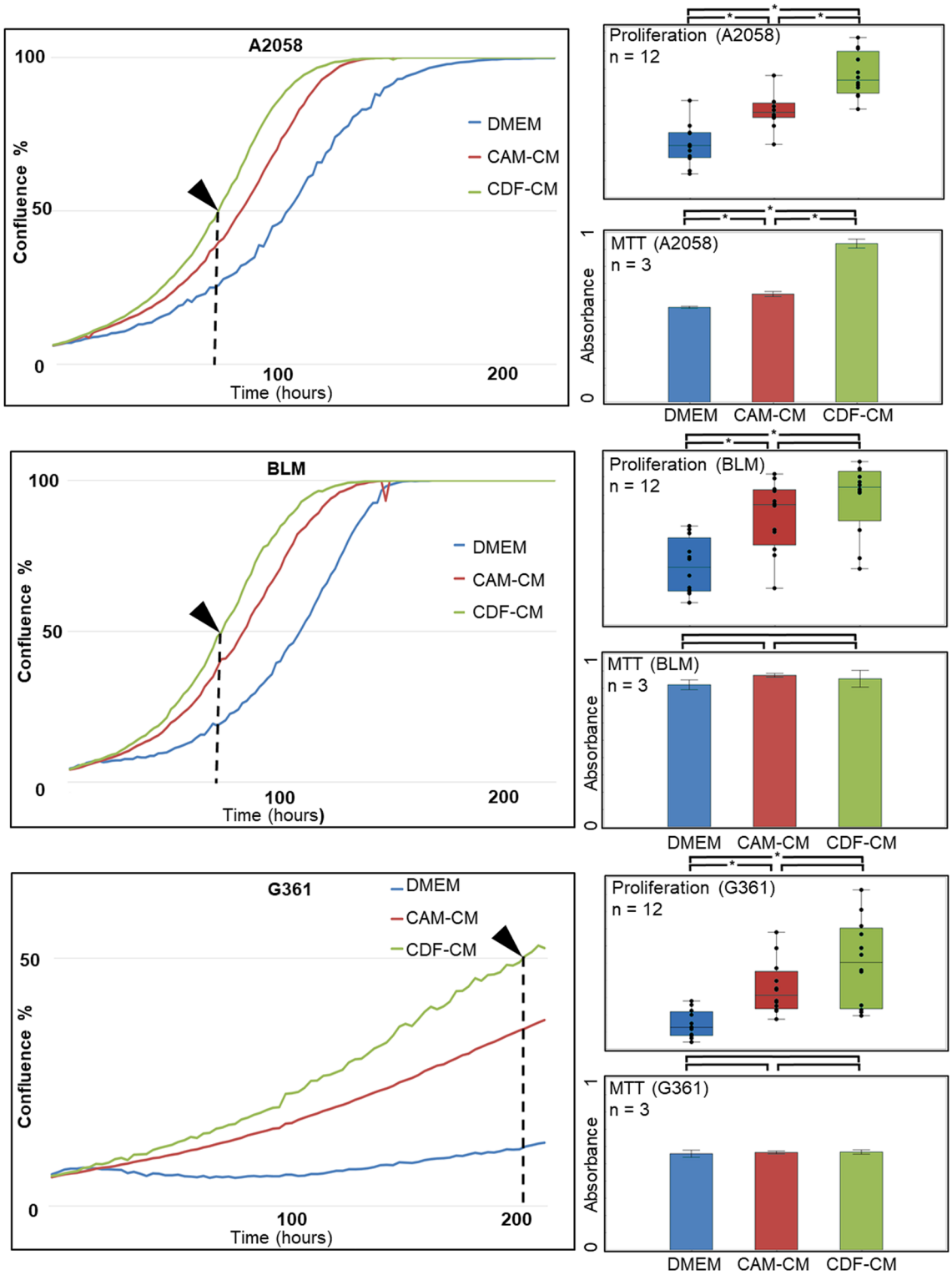

Fig. 3 Proliferation curves of A2058, BLM and G361 treated with DMEM, CAM-CM and CDF-CM, respectively. Each curve was plotted as a mean value of % confluence from independent stable reference observation points ($n = 12$) using the IncuCyte life cell analysis system. The cell proliferation was compared under different culture conditions (DMEM vs CAM-CM vs CDF-CM) at the time when the first curve met 50% confluence value (arrowhead) using the Tukey's Honest Significance test. Significant comparisons are indicated by asterisks ($p < 0.05$). The metabolic activity of cells under different culture conditions (DMEM vs CAM-CM vs CDF-CM) was evaluated using the MTT test ($n = 3$ for each condition). The significance of results was tested using the Tukey's Honest Significance test. Significant comparisons are highlighted by asterisks ($p < 0.05$)

were easy to see due to their increased opacity on CAM *in ovo* under a low-power microscope. The melanoma cells formed very small, grouped colonies at the initial stages of the experiment (day 2, Fig. 4a–d). The layer of vessels was visualised by injected Indian ink (Fig. 4a). The identity of melanoma cells was also confirmed by immunocytochemical detection of vimentin (Fig. 4b, c, red signal, Vim). This staining documented the presence of cancer cells on the surface of CAM above the vessels by accumulation of DAPI-positive nuclei. Furthermore, we performed X-ray micro-CT of the vessels injected with resin or PTA (Fig. 4d). All these methods supported the intimate relationship between the vessels and tumour cells during the initiation of melanoma growth on the CAM surface.

In later stages of the experiment (day 6), we observed more extensive opacities on the surface of CAM by the low-power microscope or even by the naked eye. These clusters were formed by the transplanted melanoma cells. This was confirmed by enzymatic X-Gal reaction on CAM whole-mount (highlighting selectively LacZ-tagged cells—Fig. 5a, bluish clusters). A similar extent of melanoma growth was confirmed by vimentin staining of untagged cells (Fig. 5b, red signal). The vascular pattern of CAM was significantly rearranged at this stage. We observed that the centripetal growth of blood vessels to the tumour site occupied by cancer cells was very well visible in specimens with resin-injected vessels (Fig. 5c). Optical visualisation of Mercox-microinjected CAM vessels demonstrated that the vessels in CAM overlaid the accumulation of tumour cells without penetration to the melanoma cell mass (Fig. 5d).

Invasion of melanoma cells into the CAM stroma was a rare event. We confirmed invasion only in two samples histologically. Vimentin staining (Fig. 6a) revealed scattered melanoma cells on the surface of CAM and also inside the CAM stroma. The second sample contained a distinct region, where tumour cells invaded from the surface into the CAM stroma and formed small clusters (Fig. 6b). Cancer cell clusters were prominent even in HE staining, and their identity was confirmed by a positive reaction for HMB-45 marker (Fig. 6c). In this case, melanoma cells were surrounded by the typical activated mesenchymal stroma of chick CAM. We did not observe the presence of any stromal elements of human origin, e.g., cancer-associated fibroblasts positive for human vimentin. The specificity of the immunohistochemical reaction was demonstrated by the negative control (Fig. 6d).

The isolated limb bud primordium (HH stages 23–24) grafted on CAM as a model of hypoxic tissue niche reshaped the vascular pattern of CAM of the acceptor eggs significantly. Under these hypoxic signals, the CAM vessels successfully penetrated the limb (Fig. 7a).

Consequently, we observed further development of the grafted limb during the experiment, confirming the viability

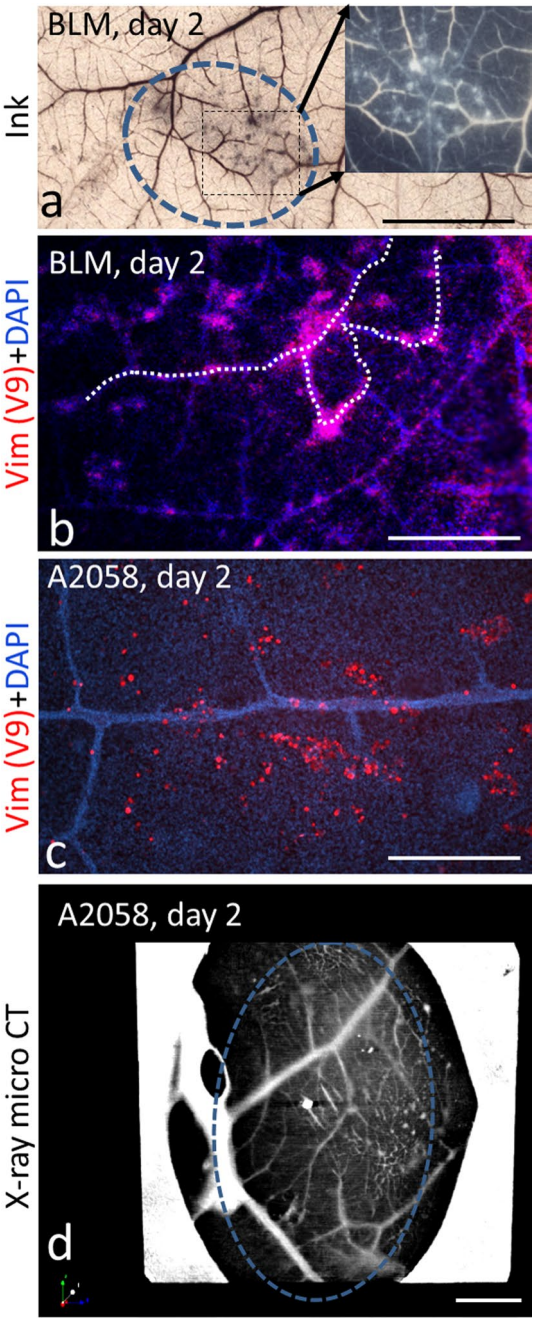

Fig. 4 Chick CAM 2 days after application of BLM (**a**, **b**) and A2058 melanoma cells (**c**, **d**) after intravascular injection of vessels by India ink in the bright and dark field (**a**). The melanoma cells are positive for human vimentin (red signal, **b**, **c**). The nuclei of melanoma cells and CAM cells are stained blue by DAPI (**b**, **c**), the white dashed line highlighted course of more prominent vessel. Similar area after injection of PTA is visualised by X-ray micro-CT in (**d**). Bar is 100 (**a**–**c**) and 500 (**d**) µm, respectively

of this tissue. Melanoma cells were attracted to the site of limb transplantation and surrounded the limb primordium in all studied samples (Fig. 7a, b—positive vimentin staining, red signal). However, the limb primordia were colonised

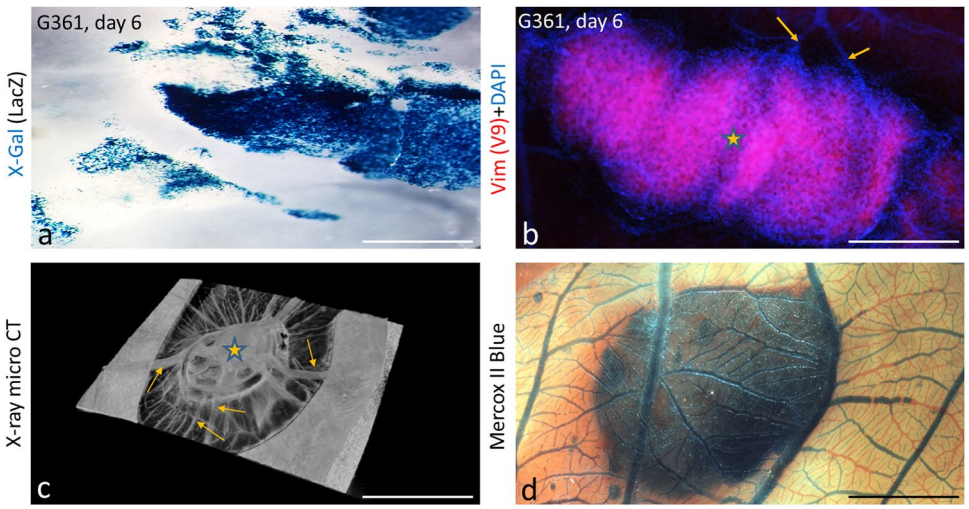

Fig. 5 Accumulation of melanoma cells on the surface of CAM 6 days after grafting (**a**—LacZ-tagged cells in bluish colour after X-Gal staining, **b**—vimentin V9-stained untagged melanoma cells in red signal (asterisk)). Chick vessels oriented to cancer cells stained blue by DAPI are marked by arrows (**b**). Similar site after injection of resin demonstrates blood vessels converging to accumulated melanoma cells (arrows, c). Inspection of a similar site by optical microscope demonstrates that blood vessels cross under the tumour inside the CAM and do not penetrate to the tumour mass (**d**). Bar is 50, 500 and 1000 µm, respectively

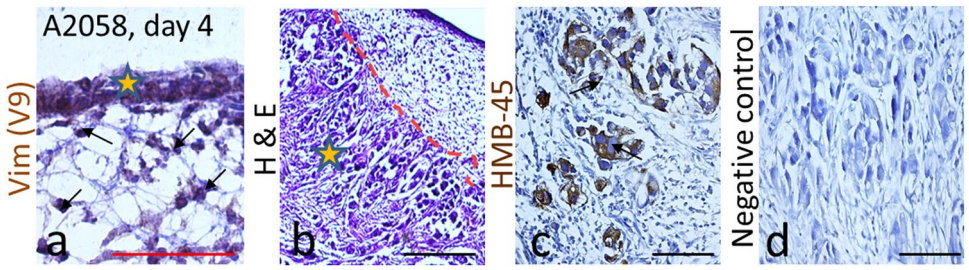

Fig. 6 Section of CAM. Melanoma cells (asterisk) are located on the CAM surface with sporadic human vimentin-positive cells in the stroma (**a**). In a single case only, we observed solid melanoma (asterisk) in the CAM stroma (**b**). These cells were positive for melanocyte marker HMB-45 (**c**). Bar is 100 and 300 µm, respectively

by melanoma cells only in two cases, in both of them in the perichondrium covering the anlage of digits (Fig. 7c). The identity of these colonising melanoma cells was confirmed by positive detection of the HMB-45 marker (negative control is presented in Fig. 7d).

We did not observe melanoma cells localised in the internal organs (liver, lung, brain) of the embryos through the interval of 5–6 days after melanoma cell transplantation by immunohostochemistry. We present the summary of all our xenotransplantation experiments in Table 1.

Discussion

This study shows that CAM in the chicken embryo offers an attractive in vivo biological substrate for the study of melanoma cell behaviour.

It is evident that any fibroblast-conditioned media used in our experiment significantly enhanced the proliferation of melanoma cells when compared to standard culture media. This observation highlights the dependence of melanoma proliferation on the microenvironmental cues represented here by fibroblast-secreted molecules (e.g., growth factors, chemokines, cytokines, etc.). The topic was recently reviewed by several authors (Lacina et al. 2018; Plzák et al. 2019; Strnadová et al. 2019). Among most likely candidates, IL-6, IL-8, CXCL-1, EGF, bFGF, HGF, and VEGFA play an essential role in cancer cell biology. We demonstrated in our previous work that IL-6 and IL-8 can influence invasiveness of melanoma cells in vitro (Jobe et al. 2018), and increased production of IL-6 by the cancer ecosystem stimulates patient cancer-dependent wasting and cachexia, as reviewed by Lacina et al. (2019). A similar trend was evident and reached

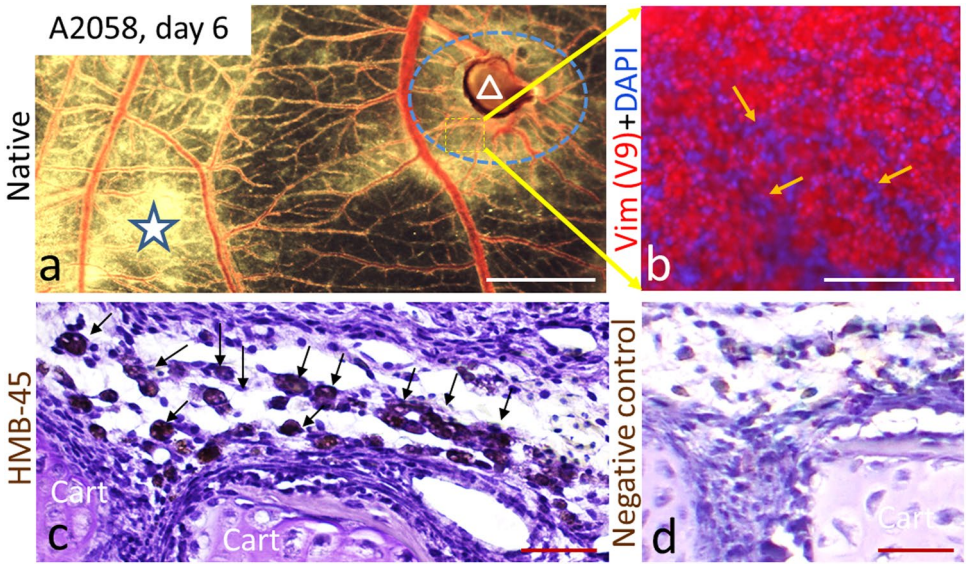

Fig. 7 Site of melanoma cell application (**a**—asterisk) and movement of melanoma cells to the grafted limb bud (**a**—triangle). When the specimen was stained as a whole-mount preparation by human vimentin (detail of the dashed quadrangle, vimentin in red signal), numerous positive cells were detected. A dense capillary network in the CAM is present at this site (**b**, yellow arrows). In the tissue section of the grafted limb primordium, the melanoma cells express specific marker HMB-45 (brown signal) in the vicinity of the cartilaginous digit primordia of the autopodial region of the limb (Cart, **c**, **d**). Bar represents 50, 100 and 1000 µm, respectively

statistical significance in all three studied cell lines. This was evident even in the case of embryonic CAM compared to pure DMEM. However, their adult CDF counterparts promoted melanoma proliferation somewhat more efficiently. This is a severe warrant to all those who use in vitro models, because employment of any complex biological material (represented here by the conditioned medium) can be potentially misleading. In such a case, a trivial comparison with pure DMEM would inevitably lead to statistically significant but biologically inappropriate conclusions.

Nevertheless, we confirmed the statistical significance of CAM vs CDF conditioned media only in the case of A2058 cell line proliferation (p value 0.002). In BLM and G361 melanoma cell lines, the trend of growth was similar, yet not statistically significant. The MTT test of metabolic activity in melanoma cells again confirmed the significant differences for A2058 melanoma in conditioned media only (p value less than 0.001). The differences observed in BLM and G361 were also insignificant.

Similarly to adult chicken fibroblasts, the chicken embryonic cells produce many factors mentioned earlier, including IL-6, IL-8, VEGFA (Xing and Schat 2000; Kosla et al. 2013), and their production can be stimulated, e.g., by heating or infection. These data can explain the stimulatory effect of both types of chicken fibroblasts on melanoma cell growth in comparison with non-conditioned media, but they are unable to elucidate the difference between both types of chicken fibroblasts.

Our data confirmed the tested melanoma cell lines as suitable candidates for further research focusing on the inhibitory effect of the embryonic microenvironment. However, the A2058 cell line is the most sensitive for further research in model embryo. This phenomenon was noted by various embryologists earlier and reviewed extensively in recent years by Kasemeier-Kulesa and Kulesa (2018). This evidence acquired with A2058 can help us to understand the switching on/off effect of the embryonic microenvironment on the phenotype and malignant behaviour of cancer cells. The embryonic microenvironment seems to be able to overdrive the tumour cell malignant potential, presumably by epigenetic mechanisms (Abbott et al. 2008). Isolated embryonic stem cells and their products can also attenuate the malignant properties of melanoma cells (Kim et al. 2011; Kodet et al. 2013). Moreover, cancer cells can enter apoptotic death after contact with specific embryonic proteins (Cucina et al. 2006). The inhibitory effect of embryonic fibroblasts on the metabolism of melanoma cells seems to be therapeutically relevant, because cell metabolism may represent a potential therapeutic target (Kroemer and Pouyssegur 2008). This proof of concept was demonstrated by the therapeutic manipulation of mitochondria in cancer cells (Kalyanaraman et al. 2018). Similar results were observed in multiple types of tumours.

Kain et al. (2014) reviewed the plausibility of CAM employment in cancer studies. The data regarding melanoma cell growth on CAM are somewhat limited. However, sparse are these data, they often support our observations

(Jayachandran et al. 2015; Avram et al. 2017). Unequivocally, we can also confirm that melanoma cells successfully adhere to CAM covering larger vessels. The tumour cell clusters consequently stimulate the centripetal growth of vessels to the engraftment site. Others have also reported stimulation of the centripetal growth of vessels to cancer cell grafting (Ribatti 2008; Nowak-Sliwinska et al. 2014, 2018). Notably, we have not detected any evident penetration of the vessels to the melanoma cell mass.

On the other hand, this oriented vessel rearrangement and growth is not tumour specific, as the limb bud grafted on CAM also stimulates this patterning. Under these hypoxic signals, CAM vessels can even penetrate to the grafted limb bud. Given by this remarkable capacity for vascular growth, CAM is, therefore, traditionally used as a suitable tool for vascular biology. These observations could indicate the sustainability of the CAM-based model for studying the melanoma neovascularisation. However, we have not detected any sign of intravascular invasion or any distant metastatic involvement in our experimental models. We assume that this should be considered with precaution if these applications are intended for melanoma research.

Local invasion is another clinically relevant aspect of melanoma that is worthy of study on the CAM model. The invasive potential of cancer cells in CAM experiments was reported with a variable rate of frequency of success. Based on our results, engrafted melanoma cells invaded into the stroma of CAM slowly and only to a minimal extent. All three cell lines used in our study revealed otherwise highly invasive behaviour in various traditional assays (e.g., in Boyden chambers). We were able to confirm the aggressive growth of tumour to CAM only in two samples. Although others do not emphasise this aspect, it seems that the invasion of tumour cells into the CAM stroma is generally rare when tumour cell suspension is used (Deryugina and Quigley 2008; Subauste et al. 2009). This invasiveness seems to be enhanced by upregulation of the histone methyltransferase EZH2 expression in cancer cells (Liu et al. 2013a, b). When minced tumour mass is transplanted to CAM instead of cell suspension, the infiltrative growth of cancer cells to the CAM stroma is more frequently observed (Ghaffari-Tabrizi-Wizsy et al. 2019). This underscores the essential role of the supportive cancer microenvironment in tumour cell invasiveness.

Of note, melanoma cells on CAM usually formed only aggregates of tumour cells without the presence of any stroma. However, when they rarely invaded the CAM, the stroma originated from the local CAM mesenchyme was well developed. Furthermore, the tissue landscape may also mechanistically enhance the melanoma cell invasion in CAM. It was proposed that the external stealth of blood vessels may serve as a possible pathway for the malignant cell migration (Lugassy and Barnhill 2007).

Finally, the solid organ metastasis after cancer cell transplantation in the chick embryo assays is believed to be exceedingly rare (Kalirai et al. 2015; Herrmann et al. 2018). Unequivocally, we confirmed no organ metastases observed by us in the embryos after application of melanoma cells to CAM in the presented study by immunohistochemical methods. On the other hand, the limb bud successfully grafted to CAM was able to attract migration of melanoma cells, which formed a distinct halo surrounding the graft. Nevertheless, only exceptional melanoma cells were detected histologically inside the grafted limb. PCR based methods might offer highly sensitive tools if detection of rare metastatic cells would be the primary target of interest (Zijlstra et al. 2002). More specifically, the ALU PCR technique (Cardeli 2011) allows highly sensitive identification of a very limited number of heterogeneous cells in the dominant cell mass (Funakoshi et al. 2017). Thus, ALU PCR can easily accompany morphological methods to detect the rare metastatic cells of human origin in the host embryo organs and tissues. This might be critical with respect to the limited duration of the CAM experiments. We believe that this combination can increase the CAM model potential in our future research.

Melanoma cells grafted to the chicken embryo reduced their malignant potential (Díez-Torre et al. 2009). The limited invasiveness of melanoma cells to CAM and the inhibitory effect of CAM fibroblasts on the melanoma cell growth corresponds with the observation that embryonic microenvironment/embryonic stem cells exhibit distinct anticancer effects on melanoma cells by inhibiting the PI3K/AKT pathway (Kim et al. 2010; Kodet et al. 2013; Liu et al. 2013a; Wang et al. 2019). Gremlin secreted by embryonic cells as an antagonist of BMP-4 may participate in the inhibition of melanoma cell proliferation (Kim et al. 2011). Similarly, noggin and its balance with BMP proteins and nodal may also be involved in the control of melanoma cell behaviour by the embryonic microenvironment (Burstyn-Cohen et al. 2004; Sinnberg et al. 2018). Finally, embryonic stem cells may exhibit tumoricidal properties based on the FAS/FASL mechanism (Li et al. 2018).

Conclusion

CAM represents an intriguing biological model for the study of several aspects of melanoma biology. This substrate allows research oriented on the study of malignant cell adhesion to the biological membrane. It can serve well for studies of both proliferation and migration to the source of chemoattractant or to the hypoxic site (inside the grafted limb bud). The CAM model is applicable in studies of neovascularization of the tumour bed. Alternatively, it can also be useful in the context of premetastatic niches formed within the microenvironment of a living organism. On the other

hand, no signs of intravascular invasion have been detected. Moreover, tumour cells are not able to extensively invade the CAM stroma and form an invasive tumour or distant metastasis. These limitations can be due to the time restrictions of the experiments (prior to embryo hatching) or to the specific non-permissive biological properties of CAM. The CAM microenvironment is, therefore, worthy of further research in the future. The invasion of melanoma cells to CAM represents a great challenge, because the understanding of this phenomenon can be of therapeutic relevance.

Acknowledgements This research was funded by the Ministry of Education, Youth and Sports of the Czech Republic, Operational Programme Research, Development and Education, project "Centre for Tumour Ecology—Research of the Cancer Microenvironment Supporting Cancer Growth and Spread" (reg. no. CZ.02.1.01/0.0/0.0/16_019/0000785), project National Sustainability Programme II (Project BIOCEV-FAR reg. no. LQ1604), and project BIOCEV (CZ.1.05/1.1.00/02.0109). Funding from the project "The Equipment for Metabolomics and Cell Analyses," reg. No. CZ.1.05/2.1.00/19.0400, supported by the Research and Development for Innovations Operational Programme (RDIOP) co-funded by the European Regional Development Fund and the state budget of the Czech Republic was also employed, along with support from Charles University (PROGRES Q28).

References

Abbott DE, Bailey CM, Postovit LM et al (2008) The epigenetic influence of tumor and embryonic microenvironments: how different are they? Cancer Microenviron 1:13–21

Avram S, Coricovac DE, Pavel IZ et al (2017) Standardization of A375 human melanoma models on chicken embryo chorioallantoic membrane and Balb/c nude mice. Oncol Rep 38:89–99

Bailey CM, Kulesa PM (2014) Dynamic interactions between cancer cells and the embryonic microenvironment regulate cell invasion and reveal EphB6 as a metastasis suppressor. Mol Cancer Res 12:1303–1313

Bailey CM, Morrison JA, Kulesa PM (2012) Melanoma revives an embryonic migration program to promote plasticity and invasion. Pigment Cell Melanoma Res 25:573–583

Bohn W, Wiegers W, Beuttenmüller M, Traub P (1992) Species-specific recognition patterns of monoclonal antibodies directed against vimentin. Exp Cell Res 201:1–7

Burstyn-Cohen T, Stanleigh J, Sela-Donenfeld D, Kalcheim C (2004) Canonical Wnt activity regulates trunk neural crest delamination linking BMP/noggin signaling with G1/S transition. Development 131:5327–5339

Cardeli M (2011) Alu PCR. Methods Mol Biol 687:221–229

Cimpean AM, Ribatti D, Raica M (2008) The chick embryo chorioallantoic membrane as a model to study tumor metastasis. Angiogenesis 11:311–319

Cucina A, Biava PM, D'Anselmi F et al (2006) Zebrafish embryo proteins induce apoptosis in human colon cancer cells ($CaCO_2$). Apoptosis 11:1617–1628

Deryugina EI, Quigley JP (2008) Chick embryo chorioallantoic membrane model systems to study and visualize human tumor cell metastasis. Histochem Cell Biol 130:1119–1130

Díez-Torre A, Andrade R, Eguizábal C et al (2009) Reprogramming of melanoma cells by embryonic microenvironments. Int J Dev Biol 53:1563–1568

Dvořánková B, Szabo P, Kodet O et al (2017) Intercellular crosstalk in human malignant melanoma. Protoplasma 254:1143–1150

Dvořánková B, Lacina L, Smetana K Jr (2019) Isolation of normal fibroblasts and their cancer-associated counterparts (CAFs) for biomedical research. Methods Mol Biol 1879:393–406

Funakoshi K, Bagheri M, Zhou M, Suzuki R, Abe H, Akashi H (2017) Highly sensitive and specific Alu-based quantification of human cells among rodent cells. Sci Rep 7:13202

Gaustad J-V, Simonsen TG, Andersen LMK, Rofstad EK (2017) Vascular abnormalities and development of hypoxia in microscopic melanoma xenografts. J Transl Med 15(1):241

Ghaffari-Tabrizi-Wizsy N, Passegger CA, Nebel L, Krismer F, Herzer-Schneidhofer G, Schwach G, Pfragner R (2019) The avian chorioallantoic membrane as an alternative tool to study medullary thyroid cancer. Endocr Connect EC-180431.R1

Hamburger V, Hamilton HL (1992) A series of normal stages in the development of the chick embryo. 1951. Dev Dyn 195:231–272

Herrmann A, Taylor A, Murray P et al (2018) Magnetic resonance imaging for characterization of a chick embryo model of cancer cell metastases. Mol Imaging 17:1536012118809585

Jayachandran A, McKeown SJ, Woods BL et al (2015) Embryonic chicken transplantation is a promising model for studying the invasive behavior of melanoma cells. Front Oncol 5:36

Jobe NP, Rösel D, Dvořánková B et al (2016) Simultaneous blocking of IL-6 and IL-8 is sufficient to fully inhibit CAF-induced human melanoma cell invasiveness. Histochem Cell Biol 146:205–217

Jobe NP, Živicová V, Mifková A et al (2018) Fibroblasts potentiate melanoma cells in vitro invasiveness induced by UV-irradiated keratinocytes. Histochem Cell Biol 149:503–516

Kain KH, Miller JW, Jones-Paris CR et al (2014) The chick embryo as an expanding experimental model for cancer and cardiovascular research. Dev Dyn 243:216–228

Kalirai H, Shahidipour H, Coupland SE et al (2015) Use of the chick embryo model in uveal melanoma. Ocul Oncol Pathol 1:133–140

Kalyanaraman B, Cheng G, Hardy M et al (2018) A review of the basics of mitochondrial bioenergetics, metabolism, and related signaling pathways in cancer cells: therapeutic targeting of tumor mitochondria with lipophilic cationic compounds. Redox Biol 14:316–327

Kasemeier-Kulesa JC, Kulesa PM (2018) The convergent roles of CD271/p75 in neural crest-derived melanoma plasticity. Dev Biol 444:S352–S355

Kasemeier-Kulesa JC, Teddy JM, Postovit LM et al (2008) Reprogramming multipotent tumor cells with the embryonic neural crest microenvironment. Dev Dyn 237:2657–2666

Kaufman CK, Mosimann C, Fan ZP et al (2016) A zebrafish melanoma model reveals emergence of neural crest identity during melanoma initiation. Science 29:351

Kim EY, Jeon K, Park HY et al (2010) Differences between cellular and molecular profiles of induced pluripotent stem cells generated from mouse embryonic fibroblasts. Cell Reprogram 12:627–639

Kim MO, Kim SH, Oi NZ et al (2011) Embryonic stem-cell-preconditioned microenvironment induces loss of cancer cell properties in human melanoma cells. Pigment Cell Melanoma Res 24:922–931

Klepáček I, Jirsa M (1994) Vascular pattern in the chorioallantoic membrane (CAM) after laser/photosenzitive compound treatment. I. Macroscopical findings. Folia Biol (Praha) 40:141–147

Klepáček I, Seichert V, Stingl J (1986) Ultrastructure of the peripheral vascular network of the wing of the chick embryo between the second and eight day of incubation (HH Stages 18-31). Folia Morphol (Praha) 34:346–351

Klepáček I, Peterka M, Jirsa M (1999) The embryotoxicity of PDT sensitizers (Mesoporphyrin IX, Protoporphyrin IX) before and after light irradiation in chicken embryo. In Berger J (ed) Cells. KOPP České Budějovice pp 78–79

Kodet O, Dvořánková B, Krejčí E et al (2013) Cultivation-dependent plasticity of melanoma phenotype. Tumour Biol 34:3345–3355
Kodet O, Lacina L, Krejčí E et al (2015) Melanoma cells influence the differentiation pattern of human epidermal keratinocytes. Mol Cancer 14:1
Kokorin IN, Gudima OS (1968) An electron microscopic study of D. sibiricus contrasted with phosphowolframic acid. Zh Mikrobiol Epidemiol Immunobiol 45:5–8 **(in Russian)**
Kolesová H, Bartoš M, Hsieh WC et al (2018) Novel approaches to study coronary vasculature development in mice. Dev Dyn 247:1018–1027
Kong BW, Lee JY, Bottje WG et al (2011) Genome-wide differential gene expression in immortalized DF-1 chicken embryo fibroblast cell line. BMC Genom 12:571
Kosla J, Dvorak M, Cermak V (2013) Molecular analysis of the TGF-beta controlled gene expression program in chicken embryo dermal myofibroblasts. Gene 513:90–100
Kroemer G, Pouyssegur J (2008) Tumor cell metabolism: cancer's Achilles' heel. Cancer Cell 13:472–482
Lacina L, Plzak J, Kodet O et al (2015) Cancer microenvironment: what can we learn from the stem cell niche. Int J Mol Sci 16:24094–24110
Lacina L, Kodet O, Dvořánková B, Szabo P, Smetana K (2018) Ecology of melanoma cells. Histol Histoathol 33:247–254
Lacina L, Brábek J, Král V, Kodet O, Smetana K Jr (2019) Interleukin-6: a molecule with complex biological impact in cancer. Histol Histopathol 34:125–136
Lee LM, Seftor EA, Bonde G et al (2005) The fate of human malignant melanoma cells transplanted into zebrafish embryos: assessment of migration and cell division in the absence of tumor formation. Dev Dyn 233:1560–1570
Li Y, Fan Y, Xu J et al (2018) Genome-wide RNA-Seq identifies Fas/FasL-mediated tumoricidal activity of embryonic stem cells. Int J Cancer 142:1829–1841
Liu J, Huang Z, Yang L et al (2013a) Embryonic stem cells modulate the cancer-permissive microenvironment of human uveal melanoma. Theranostics 9:4764–4778
Liu M, Scanlon CS, Banerjee R et al (2013b) The histone methyltransferase EZH2 mediates tumor progression on the chick chorioallantoic membrane assay, a novel model of head and neck squamous cell carcinoma. Transl Oncol 6:273–281
Lugassy C, Barnhill RL (2007) Angiotropic melanoma and extravascular migratory metastasis: a review. Adv Anat Pathol 14:195–201
Navarro M, Carretero A, Canut L et al (1998) Injection technique and scanning electron microscopic study of the arterial pattern of the 20 gestation days (G20) rat fetus. Lab Anim 32:95–105
Nowak-Sliwinska P, Segura T, Iruela-Arispe ML (2014) The chicken chorioallantoic membrane model in biology, medicine and bioengineering. Angiogenesis 17:779–804
Nowak-Sliwinska P, Alitalo K, Allen E et al (2018) Consensus guidelines for the use and interpretation of angiogenesis assays. Angiogenesis 21:425–532
Pérez-Guijarro E, Day CP, Merlino G et al (2017) Genetically engineered mouse models of melanoma. Cancer 123(S11):2089–2103
Plzák J, Bouček J, Bandúrová V et al (2019) The head and neck squamous cell carcinoma microenvironment as a potential target for cancer therapy. Cancers 11:440
Ribatti D (2008) Chick embryo chorioallantoic membrane as a useful tool to study angiogenesis. Int Rev Cell Mol Biol 270:181–224
Ribatti D (2014) The chick embryo chorioallantoic membrane as a model for tumor biology. Exp Cell Res 328:314–324
Ribatti D (2016) The chick embryo chorioallantoic membrane (CAM). A multifaceted experimental model. Mech Dev 141:70–77
Rugh R (1948) Experimental embryology. A manual of techniques and procedures. Burgess Publishing Comp, Minneapolis
Shakhova O (2014) Neural crest stem cells in melanoma development. Curr Opin Oncol 26:215–221
Sinnberg T, Levesque MP, Krochmann J et al (2018) Wnt-signaling enhances neural crest migration of melanoma cells and induces an invasive phenotype. Mol Cancer 17:59
Stockert JC, Horobin RW, Colombo LL et al (2018) Tetrazolium salts and formazan products in cell biology: viability assessment, fluorescence imaging, and labeling perspectives. Acta Histochem 120:159–167
Strnadova K, Sandera V, Dvorankova B et al (2019) Skin aging: the dermal perspective. Clin Dermatol 37:326–335
Subauste MC, Kupriyanova TA, Conn EM et al (2009) Evaluation of metastatic and angiogenic potentials of human colon carcinoma cells in chick embryo model systems. Clin Exp Metastasis 26:1033–1047
Tomiyama L, Kamino H, Fukamachi H, Urano T (2017) Precise epitope determination of the anti-vimentin monoclonal antibody V9. Mol Med Rep 16(4):3917–3921
Wang C, Wang X, Liu J et al (2019) Embryonic stem cell microenvironment suppresses the malignancy of cutaneous melanoma cells by down-regulating PI3K/AKT pathway. Cancer Med 8:4265–4277
Xing Z, Schat KA (2000) Expression of cytokine genes in Marek's disease virus-infected chickens and chicken embryo fibroblast cultures. Immunology 100:70–76
Zijlstra A, Mellor R, Panzarella G et al (2002) A quantitative analysis of rate-limiting steps in the metastatic cascade using human-specific real-time polymerase chain reaction. Cancer Res 62:7083–7092
Živicová V, Lacina L, Mateu R et al (2017) Analysis of dermal fibroblasts isolated from neonatal and child cleft lip and adult skin: developmental implications on reconstructive surgery. Int J Mol Med 40:1323–1334